

# Robust-fidelity atom-photon entangling gates in the weak-coupling regime

Ying Li,<sup>1</sup> Leandro Aolita,<sup>2</sup> Darrick E. Chang,<sup>2</sup> and Leong Chuan Kwek<sup>1,3,4</sup>

<sup>1</sup>*Centre for Quantum Technologies, National University of Singapore, Singapore 117543*

<sup>2</sup>*ICFO-Institut de Ciències Fotòniques, Parc Mediterrani de la Tecnologia, 08860 Castelldefels (Barcelona), Spain*

<sup>3</sup>*Institute of Advanced Studies (IAS), Nanyang Technological University, Singapore 639673*

<sup>4</sup>*National Institute of Education, Nanyang Technological University, Singapore 637616*

(Dated: May 17, 2022, version 2)

We describe a simple entangling principle based on the scattering of photons off single emitters in one-dimensional waveguides (or extremely-lossy cavities). The scheme can be applied to photonic qubits encoded in polarization or time-bin, and features a filtering mechanism that works effectively as a built-in error-correction directive. This automatically maps imperfections from weak couplings, atomic decay into undesired modes, frequency mismatches, or finite bandwidths of the incident photonic pulses, into heralded losses instead of infidelities. The scheme is thus adequate for high-fidelity maximally entangling gates even in the weak-coupling regime. These, in turn, can be directly applied to store and retrieve photonic-qubit states, thereby completing an atom-photon interface toolbox, or to sequential measurement-based quantum computations with atomic memories.

PACS numbers: 03.67.-a,42.50.Pq,42.50.Ct

*Introduction.*— Optical-to-near-infrared photons constitute the most natural system to transport qubits (quantum bits) [1]. They have been dubbed “flying qubits” for the ease with which they can be sent to distant locations. On the other hand, due to their stability and relatively-long coherence properties, atoms readily offer an excellent physical realization of “stationary qubits”. Controlled interactions between photons and atoms [2] are thus crucial for long-distance quantum communication (QC) or, more generically, quantum networking [3]. In this respect, maximally entangling gates play a special role: They are used for state-transfer from atoms to photons [4], or vice versa [3]; to entangle distant atoms via flying photons [3, 5], or different flying photons via atoms [6]; and, ultimately, for measurement-based quantum computations sequentially distributed among hybrid atomic-photonic systems [7, 8].

The dominant approach in single-atom-single-photon interaction has focused mainly on the *strong-coupling regime*, in particular for atoms in high-finesse optical cavities [2–6]. In this regime, the coherent interaction between the atom and the cavity mode strongly dominates over all other processes, including cavity leakage and atomic decay. However, despite the remarkable progress [2–6], the strong-coupling regime remains challenging for single cavity-emitter setups and poses a formidable challenge for cascaded arrangements, as would be required in quantum networks. An alternative approach consists of exploiting the so-called *Purcell regime* [9], where the cavity-atom coupling is much stronger than the atomic decay rate, but not the cavity-loss rate. The cavity is then typically referred to as a *bad cavity*, with an enhancement of the atomic spontaneous-emission rate into the cavity-output mode as the main effect (the Purcell effect), instead of coherent interactions. This particular form of *weak-coupling regime* is less technically demanding than the strong-coupling regime and can still allow for interesting state-manipulations [9].

In fact, this is exploited in a recent proposal [10] where a single quantum emitter is coupled to a one-dimensional (1D) waveguide, which can be thought of as a cavity in the limit of infinite losses, exhibiting tight transverse field confinement. This confinement induces a strong emitter-field coupling, which, it turns out, can yield very high Purcell factors  $P$ —indicating the system operates deep in the Purcell regime—[10]. With this, entanglement between flying photons and stationary emitters can in principle be created via resonant 1D scattering [11, 12] in the waveguide. This promising idea has several potential implementations, including atoms coupled to microscopic hollow fiber cores [13] or ultra-thin optical nanofibers [14], or artificial solid-state emitters, such as quantum dots [15] or nitrogen-vacancy centers [16], coupled to photonic nanowires or waveguides in photonic crystals. Nonetheless, due to emitter decay and finite coupling strengths, all physical setups are restricted to finite  $P$ . Moreover, the scattering quality is in addition affected by non-zero photonic bandwidths or detunings, and so is the absorption probability, so that the scattering event may not even take place at all. These imperfections impose fundamental limitations to 1D-scattering-based approaches.

In this paper, we propose a practical scheme for single-emitter-single-photon interfacing that circumvents these limitations. The dominant physical errors are mapped into heralded photon losses instead of computational errors. This is achieved with a particular scattering process that changes the polarization of photons, so that non-scattered photons are automatically discarded through polarization filtering. Furthermore, even for faulty processes, e.g. operating at low  $P$ , we find that the correct-polarization output photons imprint a phase in the internal state of the emitter. We show how to exploit this for maximally-entangling gates between stationary qubits encoded in the ground states of optical emitters in 1D waveguides and flying qubits encoded either in the polar-

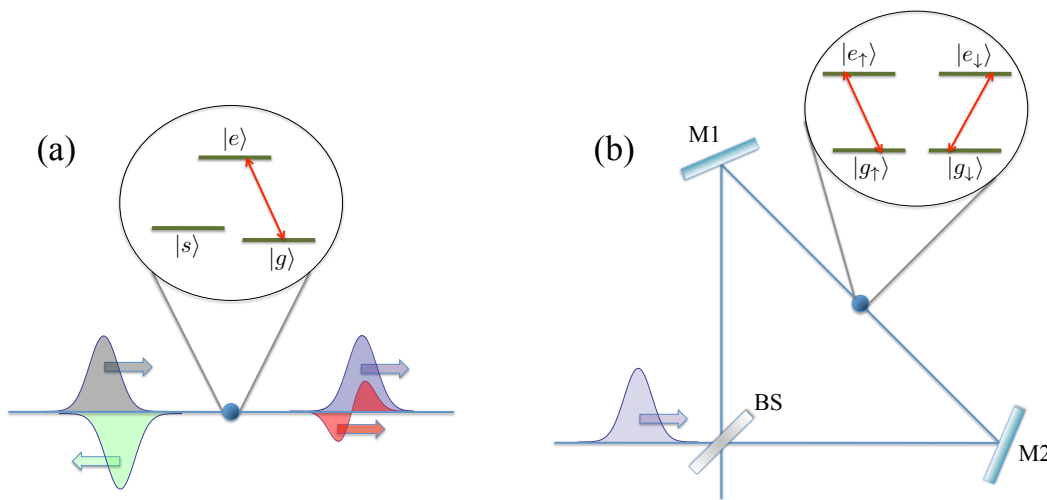


FIG. 1: Different 1D scattering setups. (a) The original arrangement [10] uses a three-level emitter, with levels  $|g\rangle$  and  $|e\rangle$  coupled via the waveguide, and a third metastable level  $|s\rangle$  coupled to  $|e\rangle$  only via classical fields. In an ideal situation, an incident photon (black) is fully reflected (green), for  $|g\rangle$ , or goes freely through (blue), for decoupled state  $|s\rangle$ . In a faulty scattering though, there is a transmitted component (red) even for  $|g\rangle$ . (b) In the present setup the scatterer has two-fold degenerate ground and excited states  $|g_\pm\rangle$  and  $|e_\pm\rangle$ , respectively, coupled by parallel transitions through orthogonally polarized photons. Even for imperfect scattering processes, if the photon is output with the correct polarization, a high-fidelity phase gate is successfully applied on the emitter. A detection of an incorrectly polarized output, on the other hand, heralds a failure. A 50/50 beam-splitter (BS) and two mirrors (M1 and M2) maximize the probability of success (see text).

ization or the time-of-arrival (time-bin [17]) of photons. In addition, the gates allow for the storage or retrieval of flying-qubit states, as well as for measurement-based quantum computations sequentially distributed among the single-emitter quantum memories.

*Photons scattering off two-level emitters in 1D.*— A two-level emitter, with ground and excited states  $|g\rangle$  and  $|e\rangle$ , respectively, dipole-coupled to a 1D continuum of electromagnetic modes can, ideally, act as a perfect mirror for resonant single photons [12]. Specifically, when the excited state is decoupled from any additional channels, an incident photon centered in a narrow bandwidth around resonance is fully reflected as a result of the destructive interference between the reemitted and the (non-absorbed) incident wavefunctions. More technically, we say that for an incident photon in a state  $|\Psi\rangle = \int dz \psi(z, t) |z\rangle$ , a perfect reflection leads to  $|\bar{\Psi}\rangle \doteq -\int dz \psi(-z, t) |z\rangle$ . On the other hand, a perfectly transmitted (freely propagating) photon remains in  $|\Psi\rangle = \int dz \psi(z, t) |z\rangle$ . Here,  $z$  is the spatial coordinate along the waveguide, conventionally taken as positive to the right, negative to the left, and with the origin  $z = 0$  at the atom's position;  $t$  is the time, with the origin  $t = 0$  at the scattering instant;  $|z\rangle$  is the state of a photon localized at  $z$ ; and  $\psi(z, t) \equiv \psi(t - z/c)$  is a normalized wave function, where parameter  $c$  is the photonic group velocity inside the waveguide ( $c > 0$  for photons propagating from left to right, and  $c < 0$  otherwise). The global minus sign in the definition of  $|\bar{\Psi}\rangle$  comes from the absorption and subsequent reemission.

Perfect 1D scattering can be used to create

emitter-photon qubit entanglement: Consider an extra metastable level  $|s\rangle$  decoupled from the waveguide light [10] [see Fig. 1 (a)]. A stationary qubit can then be encoded in the stable atomic manifold,  $\{|0\rangle_a \doteq |s\rangle, |1\rangle_a \doteq |g\rangle\}$ , and a flying qubit in the spatial wavefunction of single photons,  $\{|0\rangle_p \doteq |\Psi^R\rangle, |1\rangle_p \doteq |\Psi^L\rangle\}$ , where  $|\Psi^R\rangle$  and  $|\Psi^L\rangle$  represent incident wavepackets with the same waveform but propagating from left to right and viceversa, respectively. For the emitter in  $|1\rangle_a$ , a perfect reflection causes  $|\Psi^{R(L)}\rangle \rightarrow |\bar{\Psi}^{R(L)}\rangle \doteq -|\Psi^{L(R)}\rangle$ . Therefore, since  $|0\rangle_a$  is decoupled, a perfect process executes the maximally-entangling gate  $|\mu\rangle_a |\varphi\rangle_p \rightarrow (-X_p)^\mu |\mu\rangle_a |\varphi\rangle_p$ , where  $|\varphi\rangle_p$  is any photonic-qubit state,  $X_p$  the corresponding first Pauli matrix and  $\mu = 0$  or  $1$ .

In practice however, the reemitted amplitude is weaker than the incident one and cannot cancel it. There is always a transmitted part [10]. For incident state  $|\Psi\rangle$ , the photon comes out in  $|\Phi\rangle = |\Phi_t\rangle + |\Phi_r\rangle$ , with transmitted and reflected components  $|\Phi_t\rangle = \int dz \phi_t(z, t) |z\rangle$  and  $|\Phi_r\rangle = \int dz \phi_r(-z, t) |z\rangle$ , respectively, with [10–12]

$$\phi_t(z, t) = \psi(z, t) + \phi_r(z, t), \quad (1a)$$

$$\begin{aligned} \phi_r(z, t) = & -\frac{\Gamma_{1D}}{2} \int_0^{t-z/c} dt' \\ & \times e^{-i(\omega_0 - i\Gamma/2)(t-z/c-t')} \psi(0, t'). \end{aligned} \quad (1b)$$

Here,  $\Gamma \doteq \Gamma_{1D} + \Gamma'$  is the total atomic decay rate, with  $\Gamma_{1D}$  ( $\Gamma'$ ) the rate of atomic decay into the waveguide (all channels but the waveguide, e.g., emission into free space, or non-radiative dissipation), and  $\omega_0$  is the atomic transition frequency.  $|\Phi\rangle$  refers to the state-component

left in the waveguide, so it is normalized only when the Purcell factor  $P \doteq \Gamma_{1D}/\Gamma'$  is infinite. In particular, for finite  $\Gamma'$  and  $\Gamma_{1D} \rightarrow \infty$ , a Dirac delta appears in the integrand of (1b), so that  $\phi_r(z, t) = -\psi(0, t - z/c) \equiv -\psi(t - z/c) \equiv -\psi(z, t)$  and one has a perfect reflection:  $|\Phi\rangle = |\Phi_r\rangle = |\bar{\Psi}\rangle$ . Accordingly, the probability of photon loss is  $\kappa \doteq 1 - \langle \Phi | \Phi \rangle$ .

Apart from  $P$ , another relevant figure of merit is the reflection fidelity  $f \doteq -\langle \bar{\Psi} | \Phi_r \rangle$ , which measures how close to a perfect reflection the process is and can also be affected by frequency detunings or non-zero photonic bandwidths. In terms of  $P$  and  $f$ , the probability of photon transmission and reflection are given respectively by [10–12] the transmittance  $\mathcal{T} \doteq \langle \Phi_t | \Phi_t \rangle = 1 - \text{Re}(f) [2 - 1/(1 + P^{-1})]$  and the reflectance  $\mathcal{R} \doteq \langle \Phi_r | \Phi_r \rangle = \text{Re}(f)/(1 + P^{-1})$ . A maximally-entangling gate can only be obtained for  $P \rightarrow \infty$  and  $f = 1$ , because only then does one have  $\mathcal{R} = 1$  (so that  $|\Psi^{R(L)}\rangle \rightarrow -|\Psi^{L(R)}\rangle$ ). The lower  $\mathcal{R}$  is, the lower the fidelity of the resulting gate is.

As a simple example, imagine an incident photon spontaneously emitted, at rate  $\gamma$ , by a distant emitter. In this case the photon has a half-exponential waveform of bandwidth  $\gamma$ . Eq. (1b) is then immediately integrated to yield  $f = (1 + P^{-1} + \gamma/\Gamma_{1D} - i2\delta/\Gamma_{1D})^{-1}$ , where  $\delta$  is the detuning from  $\omega_0$ . Notice that even if  $P \rightarrow \infty$  and  $\delta \approx 0$ , already for  $\gamma \approx \Gamma_{1D}$ ,  $f$  (and therefore also  $\mathcal{R}$ ) decreases to 1/2. This would indeed be the case when emitter and scatterer are of the same species. More generally, this limitation is a serious drawback for short pulses, as those used for instance in time-bin qubits [1, 17].

*High-fidelity interaction from imperfect processes.*— Consider now a four-level emitter, with degenerate ground and excited states  $|g_{\pm}\rangle$  and  $|e_{\pm}\rangle$ , as depicted in Fig. 1 (b). These are coupled via parallel dipole transitions  $|g_{\pm}\rangle \leftrightarrow |e_{\pm}\rangle$ , associated to the absorption from, or emission to, the waveguide of  $\sigma^{\pm}$ -polarized photons.  $\sigma^+$  and  $\sigma^-$  denote two orthogonal polarizations, as for instance the right- and left-handed circular polarizations along the waveguide. The waveguide is taken as the atomic quantization axis. An incident photon of spatial wavefunction  $|\Psi\rangle$  and polarization  $\sigma^{\pm}$  scatters as

$$|g_{\pm}\rangle|\Psi\rangle|\sigma^{\pm}\rangle \rightarrow |g_{\pm}\rangle|\Phi\rangle|\sigma^{\pm}\rangle, \quad (2a)$$

$$|g_{\mp}\rangle|\Psi\rangle|\sigma^{\pm}\rangle \rightarrow |g_{\mp}\rangle|\Psi\rangle|\sigma^{\pm}\rangle. \quad (2b)$$

If, instead, the photon is in the linear-polarization state  $|h\rangle \doteq (|\sigma^+\rangle + |\sigma^-\rangle)/\sqrt{2}$ , transformations (2) yield

$$\begin{aligned} & |g_{\pm}\rangle|\Psi\rangle|h\rangle \rightarrow \\ & \frac{1}{2}|g_{\pm}\rangle[(|\Phi\rangle + |\Psi\rangle)|h\rangle \pm (|\Phi\rangle - |\Psi\rangle)|v\rangle], \end{aligned} \quad (3)$$

where  $|v\rangle \doteq (|\sigma^+\rangle - |\sigma^-\rangle)/\sqrt{2}$  is the vertical linear-polarization state. The scattering generates now a  $v$ -polarized component. More importantly, while for  $h$ -polarized outgoing photons nothing happens to the emitter, a state-dependent  $\pi$ -phase shift on the emitter accompanies the  $v$ -polarized component of (3). This phase shift will be the basis of our entangling gates.

To maximize the  $v$ -polarized component, the input photon is coherently split into two halves that simultaneously scatter off the emitter, incident from a different side each, as shown in Fig. 1 (b). Then, the reflected and transmitted components of each half are coherently joined all back into a single packet, which exits the BS through the same output mode it was input. Then,  $(|\Psi\rangle - |\Phi\rangle)/2 = -|\Phi_r\rangle$ , and discarding the  $h$ -polarized output from (3), one gets

$$|\varphi\rangle_a|\Psi\rangle|h\rangle \rightarrow -Z_a|\varphi\rangle_a|\Phi_r\rangle|v\rangle, \quad (4)$$

where  $|\varphi\rangle_a$  is any atomic-qubit state in the basis  $\{|0\rangle_a \doteq |g_-\rangle, |1\rangle_a \doteq |g_+\rangle\}$ . For perfect scattering processes  $|\Phi_r\rangle = -|\Psi\rangle$  and therefore the success probability  $p \doteq \langle \Phi_r | \Phi_r \rangle$  is 1. No photon is lost then. On the other hand, for imperfect processes, with  $P < \infty$ ,  $|\Phi_r\rangle \neq -|\Psi\rangle$  and output photons with  $h$  polarization are detected. These are discarded and the corresponding gate runs fail. However, the important thing is that the fidelity of gate (4) is not altered, only  $p$  is. We show next how to exploit successful  $Z_a$  gates for high-fidelity entangling schemes.

*Entangling gate for time-bin flying qubits.*— The first photonic-qubit encoding we consider is the time of arrival [17], consisting of incident pulses that arrive either at some “early” scattering time  $t_e$ , defining the state  $|\Psi_{t_e}\rangle$ , at some “later” time  $t_l > t_e$  [17], defining  $|\Psi_{t_l}\rangle$ , or in any superposition of the latter two states. The qubit basis is  $\{|0\rangle_p \doteq |\Psi_{t_e}\rangle, |1\rangle_p \doteq |\Psi_{t_l}\rangle\}$ . The final ingredient of the protocol is the application of a Hadamard gate  $H_a$  to the atomic qubit between  $t_e$  and  $t_l$ : If the photon arrives at  $t_e$ , the emitter undergoes first the  $Z_a$  and then  $H_a$ , whereas if it arrives at  $t_l$ , the order of the gates is reversed. Thus, since  $Z_a$  and  $H_a$  do not commute, the overall stationary-qubit gate is controlled by the flying qubit’s state. The composite unitary transformation is

$$U_{ap} = |0\rangle_p \langle 0| \otimes H_a \cdot Z_a + |1\rangle_p \langle 1| \otimes Z_a \cdot H_a \quad (5)$$

is local-unitarily equivalent to the well-known controlled-phase gate (6), defined below, and is therefore also a maximally-entangling gate.

*Entangling gate for polarization flying qubits.*— The other encoding considered is photon polarization. We define it by  $\{|0\rangle_p \doteq |v\rangle, |1\rangle_p \doteq |h\rangle\}$ . In this case, the active application of  $H_a$  is replaced with the passive interferometer shown in Fig. 2. First, the  $|0\rangle_p$  and  $|1\rangle_p$  components of an incident photon are spatially split by a polarizing beam splitter (PBS).  $|1\rangle_p$  goes through both PBSs 1 and 2 towards the scattering setup, whereas component  $|0\rangle_p$  is reflected up the other arm of the interferometer by PBSs 1. For unsuccessful events,  $|1\rangle_p$  exits the scattering setup with the same polarization,  $h$ . It is therefore transmitted back through PBSs 2 and 1 and detected in  $h$  as before, heralding the failure of the gate run. On the other hand, for successful  $Z_a$  gates the polarization is flipped. Since it is then  $v$ -polarized, the pulse is reflected up by PBS2, after which it is rotated back to  $|h\rangle$  by a half-wave plate (HWP). Finally,  $|0\rangle_p$  and  $|1\rangle_p$  are rejoined by PBS3. At

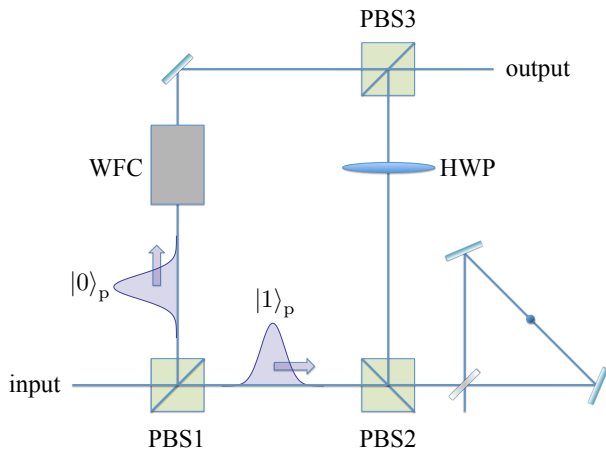


FIG. 2: Interferometric setup for polarization flying-qubits. Only component  $|1\rangle_p$  interacts with the scatterer. For successful interactions,  $|1\rangle_p$  is reflected up the interferometer by PBS2 and joins  $|0\rangle_p$  at PBS3. At the output, maximally entangling gate (6) between the flying and the stationary qubits is implemented. For unsuccessful interactions,  $|1\rangle_p$  comes back out through PBS2 and PBS1, which heralds a gate failure. Legends: PBS: polarizing BS; HWP: half-wave plate; WFC: waveform corrector. See text.

the output of PBS3, the total composite unitary transformation is the controlled-phase gate

$$U_{\text{ap}} = |0\rangle_p \langle 0| \otimes \mathbb{1}_a + |1\rangle_p \langle 1| \otimes Z_a. \quad (6)$$

For successful events of imperfect processes, i.e. where the polarization is flipped but  $|\Phi_r\rangle \neq -|\Psi\rangle$  in (4), the spatial wave functions of the packets meeting at PBS3 no longer coincide. So, unless the waveforms are matched, the output polarization qubit may be correlated with different spatial states. An experimentally relevant situation where this can be easily overcome is for incident photons with bandwidth much narrower than  $\Gamma_{1D}$ , so that  $\psi(z, t)$  can be approximated in (1b) by a plane wave. In this case the spatial waveform associated to  $|1\rangle_p$  is  $|\Phi_r\rangle \approx -k|\Psi\rangle$ , with  $|k| < 1$ . To compensate for this, a waveform corrector (WFC) in the  $|0\rangle_p$  arm maps  $|\Psi\rangle$  to  $k|\Psi\rangle$ . This slightly further decreases the overall success probability, but leaves the fidelity intact. When the photon-atom detuning  $\delta$  is zero,  $k \in [0, 1)$  and the WFC consists of an attenuator (e.g., a BS) of transmissivity  $k$ . If  $\delta \neq 0$ ,  $k \in \mathbb{C}$  and WFC simply includes also a phase modulator [18]. In the general situation  $|\Phi_r\rangle \neq |\Psi\rangle$ , WFC can be realized by a second scattering block, identical to that of Fig. 1 b), but with the emitter permanently in state  $|g_+\rangle$  (or  $|g_-\rangle$ ), preceded by a quarter waveplate to rotate  $|0\rangle_p$  to  $|\sigma^+\rangle$  (or  $|\sigma^-\rangle$ ). With this, the associated wavepacket is mapped from  $|\Psi\rangle$  to  $|\Phi_r\rangle$  without becoming entangled with the second scatterer, achieving the desired waveforms matching.

*Single-emitter quantum memories and sequential measurement-based quantum computations.*— The present maximally entangling gates, together with

single-qubit gates and measurements, allow for efficient measurement-based quantum computations sequentially distributed (by the flying qubits) among different stationary qubits of a quantum network [7, 8]. The underlying model is the seminal one-way quantum computer [23], but the approaches of [7, 8] have the advantages that (i) only the pieces of the cluster relevant for the particular computation are created (and almost immediately consumed) [8], (ii) the number of required stationary qubits is drastically smaller than in the one-way model [8], and (iii) every flying qubit needs interact with at most two stationary ones and typically with only one [7, 8].

Since these models are universal [7, 8], they include for instance the preparation of multipartite entangled states shared among different scatterers, or simply the storage, and later retrieval, of flying-qubit states, so that each emitter works as a quantum memory. The storage procedure consists essentially of maximally entangling the incident photon with the emitter, with a subsequent measurement on the outgoing photon. The retrieval, in turn, is done by maximally entangling a second photon with the emitter-qubit, in the stored state, followed by a measurement on the emitter. As a result, the second photon takes the stored state away with it.

*Feasibility.*— For quantum dots coupled to photonic-crystal waveguides,  $P > 20$  has been demonstrated [15]. This corresponds to success probabilities  $p > 0.95$ , providing thus a candidate for the implementation of the proposed schemes. In addition, the observed decay rate is  $\Gamma_{1D} > 1\text{GHz}$  [15], so that photons with pulse durations around tens of ns can scatter with excellent reflection fidelities. For the time-bin scheme, the Hadamard gate needed between the  $|0\rangle_p$  and  $|1\rangle_p$  components can be implemented in picoseconds [20]. Then, the total duration of the gate would be comparable to the coherence time of bare quantum dots [19, 20]. Nevertheless, by quantum-controlling the surrounding nuclear-spin bath, this can be enhanced by up to two orders of magnitude [21].

Another potential setup is given by atoms coupled to ultra-thin tapered optical nanofibers [14]. The modest Purcell factors ( $P \lesssim 1$ ) available there are enough to yield  $p \lesssim 0.5$ . In addition, whereas coupling single atoms to nanofibers stably is still challenging, the required techniques display a remarkably fast progress [14], and atoms readily provide coherence times as high as seconds. Finally, several groups have recently demonstrated the strong coupling of a single atom without a cavity and a tightly focused laser beam [22]. When this beam is properly mode-matched to the atomic emission, the description also resembles that of an atom interacting with a 1D waveguide.

*Conclusion and discussion*— We have proposed a simple scattering configuration for photons and optical emitters in 1D waveguides. This allows for probabilistic maximally entangling gates between stationary qubits encoded in the emitters' ground states and flying qubits encoded in photonic polarization or time-bin. The scat-

tering process tags faulty interactions with an orthogonal output polarization, which can be immediately detected and discarded, rendering a built-in error-heralding mechanism. This turns gate infidelities from weak couplings, atomic decay into undesired modes, frequency mismatches, or finite photon-pulse bandwidths, into heralded losses. The resulting gates then either succeed with perfect fidelity, or fail in a heralded manner, but are in principle never faulty. We have estimated success probabilities for realistic current-technology setups that range from  $\lesssim 50\%$  to as high as  $95\%$ .

The proposed gates apply directly to the storage or retrieval of flying-qubit states, and to measurement-based multipartite-state preparations, or generic quantum computations, sequentially distributed among distant emitters [7, 8]. As a matter of fact, for quantum information and communication applications, turning computational errors into losses is an extremely advantageous property. While the former reduce the fidelity, the latter reduce

only the efficiency, which is easier to circumvent. For example, the most optimistic thresholds of error rate per gate tolerable for fault-tolerant quantum computing are below  $3\%$  [24]. In contrast, remarkably, the one-way model [23] for quantum computation, as well [8] as the sequential counterparts considered here, can cope with particle loss rates of close to  $50\%$  [25] and heralded gate-failure rates exceeding  $90\%$  [26].

### Acknowledgments

We acknowledge financial support from the National Research Foundation & Ministry of Education, Singapore. L.A. acknowledges support from Fundaci3n Juan de la Cierva. D.E.C. acknowledges support from Fundaci3n Privada Cellex Barcelona.

- 
- [1] N. Gisin *et al.*, Rev. Mod. Phys. **74**, 1455 (2002).
  - [2] S. Haroche and J. M. Raimond, *Exploring the Quantum: Atoms, Cavities and Photons* (Oxford University Press, Oxford, United Kingdom, 2006); K. Hammerer A. S. S3rensen and E. S. Polzik, Rev. Mod. Phys. **82**, 1041 (2010).
  - [3] J. I. Cirac *et al.*, Phys. Rev. Lett. **78**, 3221 (1997); H. J. Kimble, Nature **453**, 1023 (2008); S. Ritter *et al.*, Nature **484**, 195 (2012).
  - [4] J. McKeever *et al.*, Nature **425**, 268 (2004); M. Keller *et al.*, Nature **431**, 1075 (2004); T. Wilk *et al.*, Phys. Rev. Lett. **98**, 063601 (2007).
  - [5] D. L. Moehring *et al.*, Nature **449**, 68 (2007).
  - [6] T. Wilk *et al.*, Science **488**, 317 (2007); B. Weber *et al.*, Phys. Rev. Lett. **102** 030501 (2009); N. H. Lindner and T. Rudolph, Phys. Rev. Lett. **103**, 113602 (2009); Y. Li, L. Aolita, and L. C. Kwek, Phys. Rev. A **83**, 032313 (2011).
  - [7] J. Anders *et al.*, Phys. Rev. A **82**, 020301(R) (2010); E. Kashefi *et al.*, Electron. Notes Theor. Comput. Sci. **249**, 307 (2009).
  - [8] A. J. Roncaglia *et al.*, Phys. Rev. A **83**, 062332 (2011).
  - [9] See E. Waks and J. Vuckovic, Phys. Rev. Lett. **96**, 153601 (2006); A. Auff3ves-Garnier *et al.*, Phys. Rev. A **75**, 053823 (2007); C. Bonato *et al.*, Phys. Rev. Lett. **104**, 160503 (2010); and references therein.
  - [10] D. E. Chang *et al.*, Nature Phys. **3**, 807 (2007).
  - [11] K. Kojima *et al.*, Phys. Rev. A **68**, 013803 (2003).
  - [12] J. T. Shen, and S. Fan, Opt. Lett. **30**, 2001 (2005).
  - [13] C. A. Christensen *et al.*, Phys. Rev. A **78**, 033429 (2008); M. Bajcsy *et al.*, Phys. Rev. Lett. **102**, 203902 (2009).
  - [14] G. Sagu3 *et al.*, Phys. Rev. Lett. **99**, 163602 (2007); E. Vetsch *et al.*, Phys. Rev. Lett. **104**, 203603 (2010).
  - [15] J. Claudon *et al.*, Nature Photon. **4**, 174 (2010); T. Lund-Hansen, *et al.*, Phys. Rev. Lett. **101**, 113903 (2008).
  - [16] T. M. Babinec *et al.*, Nature Nanotech. **5**, 195 (2010)
  - [17] J. Brendel *et al.*, Phys. Rev. Lett. **82**, 2594 (1999).
  - [18] In addition, the WFC may also include a delay to make  $|0\rangle_p$  arrive simultaneously with  $|1\rangle_p$  at PBS3.
  - [19] J. R. Petta *et al.*, Science **309**, 2180 (2005).
  - [20] J. Berezovsky *et al.*, Science **320**, 349 (2008).
  - [21] D. J. Reilly *et al.*, Science **321**, 817 (2008); G. de Lange *et al.*, Sci. Rep. **2:382**, DOI:10.1038/srep00382 (2012).
  - [22] B. Darqui3 *et al.*, Science **309**, 454 (2005); M. K. Tey *et al.*, Nature Phys. **4**, 924 (2008); G. Wrigge *et al.*, Nature Phys. **4**, 60 (2008); G. H3t3t *et al.*, Phys. Rev. Lett. **107**, 133002 (2011).
  - [23] R. Raussendorf and H. J. Briegel, Phys. Rev. Lett. **86**, 5188 (2001).
  - [24] E. Knill, Nature **434**, 39 (2005).
  - [25] M. Varnava, D. E. Browne, and T. Rudolph, Phys. Rev. Lett. **97**, 120501 (2006).
  - [26] Y. Li *et al.*, Phys. Rev. Lett. **105**, 250502 (2010); K. Fujii and Y. Tokunaga, Phys. Rev. Lett. **105**, 250503 (2010).